Voltage evolution and electrochemical behaviour of Soil microbial fuel cells operated in different quality soils

Jakub Dziegielowski [a,b], Michele Mascia [c], Benjamin Metcalfe [b,d], Mirella Di Lorenzo [a,b,*]

[a] Department of Chemical Engineering, University of Bath, BA2 7AY Bath, UK
[b] Centre for Biosensors, Bioelectronics and Biodevices, University of Bath, BA2 7AY Bath, UK
[c] Dipartimento di Ingegneria Meccanica, Chimica e dei Materiali, Università degli Studi di Cagliari, Via Marengo 2, 09123 Cagliari, Italy
[d] Department of Electronic and Electrical Engineering, University of Bath, BA2 7AY Bath, UK

ABSTRACT

The desire for a net-zero carbon future is a key driver for innovation in renewable energy. Amongst several emerging solutions, soil microbial fuel cells (SMFCs) pose an interesting addition as a low-cost, carbon–neutral technology. A full understanding on the electro-generative processes in SMFCs has, however, yet to be achieved, hindering the technology's translation into practical applications. In this study, an in-depth investigation into the evolution of the output voltage generated by membrane-less, flat-plate SMFCs that accounts for the contribution of both the anode and cathode potential is provided for the first time, along with a study of the influence that organic matter content and porosity in soil has on voltage dynamics. Four stages in voltage evolution over time were observed, which depended on soil properties. The content of organic matter had the greatest effect, leading to an output voltage nearly-three times higher, when it increased from 10 % to 50 %. In this case, the anode potential reached a value of −450 mV, which prompted an exponential increase in the cathode potential and led to a power density of 68 mWm^{-2}. The experimental findings were used to develop a novel computational model that, by predicting the electrochemical behaviour of the SMFC in different soils, becomes a powerful guide for operating strategies that can markedly enhance electricity generation. Consequently, this study sets the foundation for effective system optimisation and real applications.

Introduction

The 21st century will go down in history as a period of transitions, pressed by the rapidly changing climate. Humans have finally begun to realise the scale of the damage inflicted on the planet, through the abusive use of fossil fuels, and there is an urgent demand to find solutions to minimise our carbon footprint whilst satisfying growing energy demands. Currently, hydro, wind and solar are the dominant forms of renewable energy, accounting for 54 %, 24 % and 21 % of the world's total renewable energy generation capacity respectively [1]. However, their climate and geographical dependencies, allow them to meet only 11.2 % of the total energy consumption [1]. To fully replace fossil fuels, additional renewable energy technologies that can work in symbiosis with nature are needed. Bio-based technologies are particularly attractive as biomass is an abundant resource [2]. Modern biomass, especially biofuels and wood pellets, are increasingly used for heat and power generation, alongside other traditional biomass sources such as agricultural by-products [3]. Additionally, new bio-based forms of energy are continually emerging, one of which is soil microbial fuel cell (SMFC) technology.

SMFCs hold great potential as a low-cost and sustainable power source [4]. The technology relies on endogenous electroactive microorganisms that convert the chemical energy stored in biodegradable matter in soil directly into electricity [5]. With respect to other types of microbial fuel cells, the complexity of soil matrices, however, introduces several unknowns in the processes behind energy generation by SMFCs. The influence on the performance of SMFC systems of moisture content, soil texture [6] and reactor design [7], has been investigated to maximise the power output and enhance the bioremediation capability. Nonetheless, to date the voltage evolution during start-up in SMFCs has not been investigated in-depth yet, resulting in start-up times that range from weeks to months [8]. The start-up time, also referred to as the enrichment process, is associated with the time required for the electroactive bacteria to acclimate and form a biofilm on the anode surface. As the electroactive biofilm grows, a charge imbalance is generated due

Nomenclature

List of symbols

Symbol	Description Units
a_j	Specific area of electrodes $17,700 m^{-1}$
C_i	Concentration of i-th species $mol\,m^{-3}$
$\mathscr{D}_i$	Free diffusivity of ith species in water $m^2 s^{-1}$
$\mathscr{D}_{i,j}$	Effective diffusivity i^{th} species in the jth domain $m^2 s^{-1}$
E_j^0	Potential for the half-maximum-rate (Equations (1), 2)V
F	Faraday's Constant $96,485\,C mol^{-1}$
I	Volumetric current density $A m^{-3}$
k_k	Specific rate of kth reaction $mol\,m^{-3} s^{-1}$
k_d	Inactivation constant for biofilm d^{-1}
K	Half-saturation constant $mol\,m^{-3}$
R	Universal constant of gases $8.314\,J mol K^{-1}$
T	Temperature K
V_j	Electric potential in the j-th domain V
z_k	Number of electrons in k^{th} reaction-

Subscripts

M_S	Suspended microorganisms
M_A	Adhered microorganisms
An	Anode
Cat	Cathode
S	Organic Substrate

Greek letters

ε	Porosity of the j-th domain-
η	Electrode over-potential V
ν	Stoichiometric coefficient -
σ	Electric Conductivity $S m^{-1}$

to electron production from microbial oxidation pathways and transfer to the electrode, making the anode more negatively charged and the cathode more positively charged. Hence an electromotive force (or voltage) is created, and a current can flow across the fuel cell [9].

The enrichment process has been widely studied in conventional (i. e., liquid) microbial fuel cells to design effective strategies that can enhance performance by promoting the growth of electroactive biofilm onto the electrode surface, and by accelerating the start-up process [10]. Solutions include: poising the electrode or fuel cell potential; operating the fuel cell in open circuit voltage (OCV) mode for a defined period of time; or applying a specific external impedance to the system. [11]. Controlling either the fuel cell potential or the anode potential exposes the microbial fuel cell to potentials not normally achievable in natural redox settings, thus providing insights on biofilm evolution, composition and behaviour [11]. Aelterman et. al., demonstrated that fixing the electrodes at a set potential can regulate the activity of electroactive species, suggesting that such technique can be used to enhance electrochemical properties of mixed-culture biofilms [12]. The practicality of such approaches in the field is, however, questionable, given the requirement of external equipment such as a potentiostat. Microbial acclimation under open or closed-circuit conditions are more compatible with field settings. The closed circuit method in particular, allows the tuning of the biofilm electrochemical properties according to the applied external load [13]. It is, however, also the slowest method; in fact the highly selective conditions imposed by low external loads delay the development of a functional biofilm [14]. To date, no in-depth investigation on the enrichment process in soil microbial fuel cells has been reported. In SMFCs, parameters such as soil structure, porosity, moisture and substrate availability can have a marked impact on performance [15]. In particular, porosity significantly affects permeability and, therefore, the mass transfer rates of the substrate towards the electrodes and its availability for the bio-electrochemical reactions [16]. Static operations, where there is no input flow of fuel, are typical in SMFCs [17]. Consequently, in these systems slow mass transfer processes can lead to local imbalances in the concentration of nutrients due to faster consumption rates at the electrode surface, markedly affecting performance over time [19]. A good prediction of the distribution of chemical species within the soil, as a function of soil properties, is therefore key to SMFC design. This information can be supported by mathematical modelling, since effective experimental determination is difficult to achieve in this case and can be very expensive.

In this study, for the first time an investigation into the evolution of the output voltage generated by flat-plate membrane-less SMFCs in different soils is performed. The soils samples differed from each other in terms of clay content, and therefore porosity, and organic content. The experimental data are used to develop a mathematical model that, by

Table 1
Physiochemical properties of the soil used in the study.

Parameter	Soil-1	Soil-2	Soil-3
pH	6.5	6.7	7
Electrical Conductivity, $\mu S cm^{-1}$	750	390	380
Nitrogen (Total), %	2.1	0.85	0.62
Phosphorous, $mg\,kg^{-1}$	510	650	770
Potassium, $mg\,kg^{-1}$	1300	1900	2400
Organic Matter, %	50	19	10
Total Organic Carbon, %	29	11	6
Clay Content	18	11	3
Silt Content	19	16	15
Sand Content	63	73	82

predicting electrochemical performance according to soil properties, becomes an important guide for the design of optimal operating conditions for SMFCs, and the consequent development of strategies for sustaining long-term performance.

Materials and methods

Materials

All reagents were purchased from Alfa Aesar and Sigma-Aldrich of analytical grade and used without further purification.

Three different soil types were used in this study, referred to as Soil-1, Soil-2 and Soil-3, which were collected from three different locations around the University of Bath campus. After collection, the soils were sieved, cleaned from small stones, roots, and leaves, and analysed (Eurofins Chemtest ltd). Table 1 summarises the properties of the three types of soil used.

The three samples differed in texture and organic content: Soil-1 and Soil-2 are sandy loams, Soil-3 is loamy sand (classification by the US department of agriculture, [20]). According to agricultural soils in England and Wales standards (data from National Soil Inventory [21], the three types of soil show organic content above mean, and clay content below mean, with Soil-3 having both values below minimum.

SMFC design and operation

The SMFC reactor design used in this study (Fig. 1a), consisted of two graphite felt electrodes (Online Furnace Services ltd), $10 \times 10 \times 0.7$ cm, at a fixed distance of 4 cm, as previously described [22]. The electrodes were manually woven with titanium wire (Alfa Aesar), which acted as the current collector. Prior to installation, the anodes underwent an acid
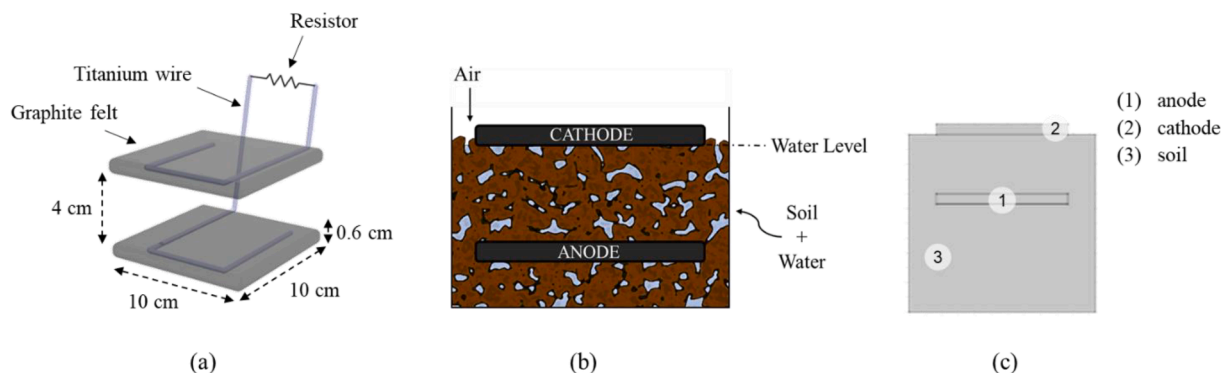
Fig. 1. (a) SMFC reactor design tested in this study: (b) Experimental set-up; (c) Schematic of the three integration domains used for the mathematical model.

and heat treatment, to increase the hydrophilicity of the graphite felt material [23]. The SMFCs were placed in PVC boxes (3 replicates per box) filled with 6 kg of soil each, with the anode buried in the soil and the cathode directly exposed to air, as shown in Fig. 1b. Three litres of water were added to each box until a water sealing layer was formed on the soil surface, which would prevent the cathodes from flooding. An additional box filled with Soil-1 was constructed to monitor the pH over time. The pH was monitored with a pH analogue sensor (DFRobot, SEN01061) logging the data every 1 min in two different depths form the soil surface: approximately at a 1 cm depth, so close to the cathode; and at a 4 cm depth, nearby the anode.

The SMFCs were operated at room temperature (i.e., 20 ± 2 °C during the day and 16 ± 2 °C during the night). A 510 Ω resistor was applied to the SMFCs and the output voltage, E, was monitored using a data acquisition system (DAQ6510, Keithley). Throughout the study, the individual electrode potential was measured once per day against a Ag/AgCl reference electrode. Every-two days, approximately 0.7 L of tap water was distributed in each box via a gravity irrigation system, comprising of a 25 L water tank (TanksDirect), an electronic water timer (Kingfisher) and a micro drip irrigation kit (Yikaich). After 57 days of operation, 50 g of biochar (5–5–5 NPK, GroChar, Carbon Gold) was added to the box with the SMFCs operated in Soil-1. The water-soluble organic compounds (WSOCs) present in the biochar [24] include similar compounds naturally found in soil dissolved organic matter, such as organic acids, sugars, amino acids, and humic substances [25], and are therefore a good nutrient source for the biofilm developed onto the surface of the anode and cathode of the SMFC. The biochar granules were ground into powder and sprinkled on top of the soil surface to maximise the release of WSOCs via a large contact area between the biochar and the irrigation wate, which would, therefore, enhance WSOCs diffusion towards the electrodes. Mixing the biochar powder into the soil would be impractical during operation as it would lead to risks of oxygen cross-contamination in the anodic region [26] and change physiochemical properties of the soil [27]. During operation, the SMFCs underwent a series of polarisation tests, performed by varying the applied resistance, R_{ext}, from 900 $k\Omega$ to 40 Ω every 10 min, by means of a resistance box (Cropico RM6 Decadcamee) and by recording the pseudo-steady output potential. Ohm's law, $E = I R_{ext}$, was used to calculate the corresponding current (I) at each value of R_{ext}. The power, P, was calculated by using the power law, $P = IE$. The internal resistance was calculated by fitting the power curves with a polynomial trend line, extrapolating the data, and applying Jacobi's law, stating that $R_{int} = R_{ext}$ at the maximum power point [28].

Model description

The SMFC behaviour was mathematically modelled to identify the different operating factors that influence the electrochemical performance and, accordingly, to derive guidelines for effective operations. The model integrates mass balance of both substrate and biomass within the soil and on the electrode surface, with the relevant equations for electrochemical and bioelectrochemical reactions, and with Poisson's equation for charge conservation, as previously reported [29]. The set of equations were solved in a 2D geometry that represents a cross-section of the experimental system. The integration domains (Fig. 1c) are: anode (domain 1), where biofilm grows and electricity is generated along with substrate consumption; cathode (domain 2), where oxygen reduction occurs along with protons consumption; soil (domain 3), where transport of chemical species occurs within the soil, which is represented as a porous matrix.

Based on the experimental results, new assumptions and features were added to the model developed previously [29], as follows:

- Microorganisms are modelled as both suspended in soil (M_s) and attached onto the electrode surface in the form of a biofilm (M_A)
- A single substrate (S) reaction is considered, where the substrate is organic matter. S is dissolved in the water within the pores of the soil. A dissolution equilibrium is established onto the pores surface between the organic matter in the dissolved (S_{eq}) and solid phase. A concentration of dissolved organic of 47 mg C dm^{-3} was assumed in particular, which corresponds to an average value reported for soil samples similar to those used in this work [30].
- At the anode, it is assumed that only bioelectrochemical reactions occur, which are catalysed by the anodic biofilm.
- At the cathode, the chemical oxygen reduction reaction (ORR) is the sole reaction initially occurring. When the anodic potential reaches a target steady value (as revealed from the experimental data), a cathodic biofilm is established so that a biologically catalysed ORR also occurs.
- Both anodic and cathodic biofilm are formed through nucleation and growth of suspended microorganisms [31]. A conduction-based kinetics is used to describe the bioelectrochemical activity of both biofilms [32] with a Nernst-Monod kinetics model, which relates substrate consumption to microbial activity and electric potential. Biofilm inactivation follows a pseudo-first order law [33,34].

Under these assumptions, the reaction rates of biofilm nucleation (r_1, mol m^{-3} s^{-1}); growth (r_2, mol m^{-3} s^{-1}); and inactivation (r_3, mol m^{-3} s^{-1}) at both anode and cathode can be written as:

$$r_1 = k_1 \frac{C_s}{C_s + K_s} \frac{C_{Ms}}{C_{Ms} + K_{s,Ms}} \left[1 + exp\left(-\frac{F}{RT}\eta_E \right) \right]^{-1} \tag{1}$$

$$r_2 = k_2 \frac{C_s}{C_s + K_s} \frac{C_{M_A}}{C_{M_A} + K_{s,M_A}} \left[1 + exp\left(-\frac{F}{RT}\eta_E \right) \right]^{-1} \tag{2}$$

$$r_3 = k_d C_{M_A} \tag{3}$$

where: k_1 (mol m^{-3} s^{-1}), k_2 (mol m^{-3} s^{-1}) and k_d (s^{-1}) are the specific reaction rates; K_s (mol m^{-3}), $K_{s,Ms}$ (mol m^{-3}), and K_{s,M_A} (mol m^{-3}) are
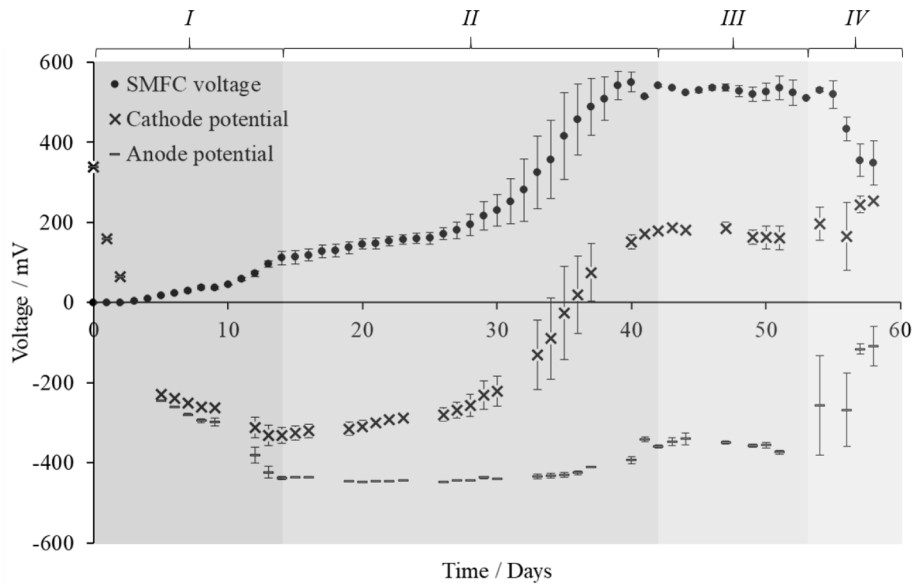
Fig. 2. Evolution of the cell voltage generated by SMFCs in Soil-1, along with cathode and anode potential vs Ag/AgCl. Error bars refer to 3 replicates.

the half saturation constants; η_E (V) is the electrode overpotential (V-E^0).

Both kinetics and diffusion processes in porous media were considered in the mass balances of the jth species in the ith domain:

$$\varepsilon_i \frac{\partial C_{j,i}}{\partial t} + \nabla \bullet \left(- \mathscr{D}_{j,i} \nabla C_{j,i} \right) = R_{j,i} \qquad (4)$$

where: $C_{i,j}$ (mol m^{-3}) is the concentration of substrate, protons, or microorganisms; ε_i is the porosity of the soil; $\mathscr{D}_{j,i}$ (m^2 s^{-1}) is the diffusivity. The reaction term $R_{j,i}$ (mol m^{-3} s^{-1}) is related to the bioelectrochemical reactions occurring onto the porous surface of the two electrodes and to the equilibrium of dissolved species in the water within the soil pores; it can be defined as:

$$R_{S,An/Cat} = -(r_1 + r_2) \qquad (5)$$

$$R_{M_S An/Cat} = -v_{OM} r_1 \qquad (6)$$

$$R_{M_A,An/Cat} = r_1 + r_2 - r_3 \qquad (7)$$

$$R_{H^+,An/Cat} = v_{H^+}(r_1 + r_2) \qquad (8)$$

$$R_{S,Soil} = a_{soil} k_s (S_{Eq} - S_{Pore}) \qquad (9)$$

where k_s, is the mass transfer coefficient of the substrate from the surface to the bulk of the pore soils: a value of 3×10^{-9} m s^{-1} was assumed for k_s, which corresponds to an average value for dissolution in stagnant water [35].

The chemical ORR at the cathode follows the Butler-Volmer-like equation [36]:

$$I_{Cat} = I_{Cat}^0 exp\left(-0.5 \frac{F}{RT} \eta_{Cat} \right) \qquad (10)$$

Charge conservation within the SMFCs is described by using Poisson's Law [37]:

$$\nabla \bullet \left(-\sigma_i \nabla V_i \right) = f_i \qquad (11)$$

where σ_i (S m^{-1}) is the conductivity and f_i (A m^{-3}) is the current source, i refers to anode (An), soil (Soil) or cathode (Cat). Equation (11) has been applied to the three domains of integration (Fig. 1c), the current sources were obtained from the rates of the faradaic (electrodes) or diffusive (soil) processes with the Faraday's law. Organic matter (the substrate) was modelled as equivalent acetate, so 8 electrons are

generated from its oxidation at the anode.

The model equations were numerically solved with the following boundary conditions:

- Soil-electrode boundaries: continuity of concentration of chemical species, and microorganisms
- External boundaries: no flux of species ($\nabla C_j = 0$) and no charge ($\nabla V = 0$).

The numerical solution was obtained by using COMSOL®, further details on model equations and numerical solution can be found in [29].

Results and discussion

Voltage evolution with time

The evolution of the voltage generated by the SMFCs over time, along with the individual electrode potentials, was measured under closed circuit conditions over a two-month period. Fig. 2 shows the results obtained. Four different stages were identified.

Stage I is associated with an increase in the output potential generated by the SMFCs, which corresponds to a decrease in the anode potential over time. Both the anode and the cathode start from a potential of + 300 mV, which, after 9 days, drops to a value of −298 mV for the anode and −262 mV for the cathode. The redox potential is indicative of how oxidised (aerobic) or reduced (anaerobic) the soil is, as well as of its electron availability. Aerated, upland soils, tend to have a positive potential of + 100 mV vs Ag/AgCl, whereas in flooded soils, as the oxygen is consumed, the potential can decline down to – 300 mV [38]. The latter case is representative of the experimental set-up in this study, since the soil moisture content was maintained above 90 % to favour the transport of ions and nutrients and minimise oxygen contamination in the anodic region.

Around day 10, a further drop of 150 mV in the anode potential can be observed (which decreased from −300 mV to −450 mV). This drop can be associated to a well enriched electroactive biofilm formation at the anode [39]. The anode potential is a consequence of the microbial-mediated redox reactions occurring at the electrode, reaching a potential set by the substrate oxidation. For example it corresponds to −487 mV in the case of acetate oxidised to CO$_2$ [40]. The large variety of chemical compounds present in soil, challenges the possibility to exactly pinpoint the substrate(s) oxidised at the anode of the SMFCs. Still, it has
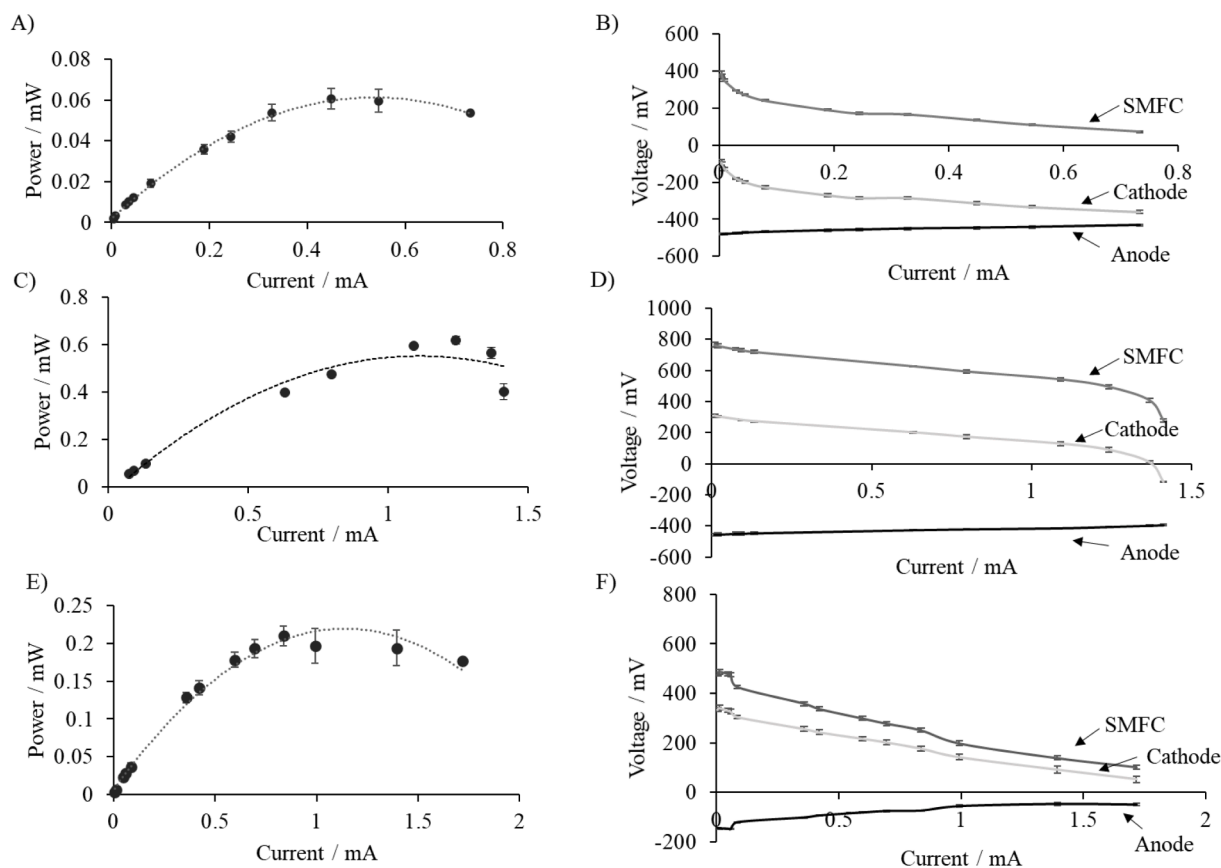
Fig. 3. Comparison of power performance at different enrichment times for SMFCs operated in Soil-1. A) Power curve and B) polarisation curve, including individual electrode potentials, after 14 days of operation. C) Power curve and D) polarisation curve, including individual electrode potentials, after 45 days of operation. E) Power curves and F) polarisation curve, including individual electrode potentials, after 60 days of operation. Error bars refer to 3 replicates.

been demonstrated that microbial fuel cells operating on a variety of substrates typically present an anode potential at open circuit of −448 mV vs Ag/AgCl [41].

At the end of the second week of operation, when the SMFCs reached a steady voltage of 110 ± 10 mV, polarisation tests were performed, as shown in Fig. 3A. Each SMFC generated a peak power of roughly 60 µW, at a current of 600 µA. Monitoring the behaviour of individual electrode potentials under different external loads revealed that the system is limited by the cathode (Fig. 3B). The anode potential remained nearly unchanged at −450 mV, suggesting no electron transfer limitations as more current was sourced from the circuit, however, the cathode potential dropped almost instantaneously from an open circuit potential of −100 mV, to nearly −400 mV, thus reflecting the voltage drop across the whole fuel cell.

Large cathode potential drops at low currents are characteristic of activation losses, and their magnitude depends on the reduction kinetics [42]. Non-modified graphite exhibits poor kinetic and electrocatalytic activity towards redox reactions. Consequently, several strategies, including acid, thermal, electrochemical, and/or microwave treatments, have been considered to enhance the electrochemical properties of the carbon electrode and its wettability [43,44]. As the cathode did not undergo the acid/heat treatment reserved for the anode, the graphite felt was hydrophobic, restricting the ionic and electrochemical interactions, resulting in very high contact resistance with the electrolyte and thus very slow oxygen reduction reaction (ORR) rates [42].

Following another 19 days of operation, the cathode potential observed an exponential increase, reaching a value as high as + 185 mV after 40 days of operation, Stage II in Fig. 2. The trend in potential growth exhibited by the cathode very closely resembles a microbial growth curve, showing a lag, an exponential and a steady-state phase,

which suggests the formation of a cathodic biofilm, responsible for decreasing the ORR activation barrier and catalysing the reduction reaction. To confirm the involvement of biological processes in the cathodic activity, biofilm enriched cathodes from sacrificial SMFCs were exposed to UV-light for 15 min. Ultraviolet treatment is an effective disinfection strategy [45], and in contrast to chemical or thermal treatments, does not affect physical and chemical properties of the electrode [46]. As shown in Fig. 1S in the Supplementary Data, the UV-treatment led to a 42 % power drop, thus confirming a biocatalytic process.

Past work into biocathodes has confirmed microbial reduction catalysis, which may follow either an anaerobic or an aerobic path, depending on the nature of the electron acceptor [47]. In this study, aerobic biocatalysis is most probable, as the cathodes are directly exposed to air. Several studies on liquid microbial fuel cells have reported the use of aerobic biocathodes, with onset potentials for ORR ranging from + 0.4 V to −0.15 V vs Ag/AgCl [48]. The highest onset potential, closely matching the observed open circuit potential of the cathode in this study (+0.32 V), was believed to be related to the activity of aerobic, electrotrophic bacteria, that gain energy for metabolism and growth by using electrons to generate ATP and to fix CO_2 into biomass [49]. Therefore, it is likely that once the anodic biofilm acclimated, and a steady electron generation occurs, the growth of an electrotrophic biofilm at the cathode is favoured, enabling a more positive cathode potential. This hypothesis would explain why the growth of the cathodic biofilm occurs only when the anode reaches a steady, negative potential. To investigate this relationship further, a side study was performed, where cathodes were replaced with fresh graphite felt electrodes, after 14 days of operation, when the anodic potential reached a value of approximately −450 mV (see Fig. 2S). Once connected to the anode via a

resistor, the cathodic potential was −281 mV, and started to incline after 5 days, taking only 2 weeks (instead of 36 days, as in Fig. 2) to reach positive potential. This finding confirms the dependency of the cathode potential evolution, on the anodic performance, and suggest a strategy to accelerate the fuel cell start-up.

After 42 days of operation, the output voltage generated by the SMFCs stabilised at 550 mV, with an anodic potential of −370 mV and a cathodic potential of + 180 mV (Stage III in Fig. 2). In this stage, both the anode and the cathode appear to be at their optimal performance, and the SMFCs generate a current four times higher than at the end of Stage I (1.1 mA vs 0.3 mA), under the fixed load. Polarisation tests confirm this result, showing a peak power 10 times greater than in Stage I, as shown in Fig. 3C. This improvement in performance is largely attributed to the cathode. As shown in Fig. 3D, the open circuit potential of the cathode significantly increased from −100 mV in Stage I to + 300 mV in Stage III. Additionally, a positive cathodic potential was sustained under lower external loads and greater currents, which suggests much greater ORR rates. The SMFCs, however, appear to be still limited by the cathode, since a sharp drop in the cathode potential, reflective of the drop in the SMFC output voltage, was observed after 1.2 mA. This performance decay, occurring at high current densities, is associated with mass transport limitation, and is referred to as cathodic concentration losses [42]. Insufficient supply of oxidants (i.e., O_2) and slow removal of products (i.e., H_2O) at the cathode are some of the causes responsible for reactant depletion or product accumulation, lowering the overall SMFC performance [42]. In microbial fuel cells, mass transport limitations at the cathode are typically much more severe than transport limitations at the anode, remaining one of the biggest barriers to power scale-up [42].

After 54 days of operation, a decay of 200 mV (over three days) was observed (Stage IV, Fig. 2). Since during this time the anode potential increased from −380 mV to −110 mV, the overall drop in the output voltage generated by the SMFCs appears to be caused by the anode. Polarisation tests further confirmed this hypothesis, as shown in Fig. 3E. The peak output power dropped by 65 %, reaching 0.2 mW, corresponding to a significant decay in the anodic performance, Fig. 3F. Although the exact cause for such behaviour is unknown, several hypotheses can be drawn from previous studies. González del Campo et. al., concluded that the build-up of thick biofilm layers onto the electrode surface, characteristic of batch systems, such as the one tested in this study, can lead to the hindrance of charge transfer to the anode, thus increasing the internal resistance and ultimately worsening the performance [50]. Further, high current generation, such as in Stage III, may force the anodic bacteria to operate beyond their metabolic capacity, eventually leading to performance collapse [51]. High current generations have also been shown to cause a marked local pH drop, as a result of proton accumulation in the anodic region, due to slower transfer kinetics, which may affect the metabolic performance of the anodic biofilm [52]. No substantial changes in the pH where, however, observed nearby the anodic and cathodic region, probably due to the limitation of the equipment used (see Fig. 3S in the supplementary Data).

Finally, this decay in performance may be caused by local fuel limitations, as a consequence of slower mass transfer rates of the organic substrate compared to kinetic rates at the anode [53]. When high current is generated, the rate of electron depletion from the anode is proportionally higher. After two weeks of operation under these conditions, the SMFCs may have reached a point where the rate of charge transfer to the anode slows down due local substrate limitation and can no longer sustain the rate of electron consumption, imposed by the external resistor, thus raising the anodic potential. A very similar trend was observed in our previous work [54]. When SMFCs were operated under maximum power point tracking, and therefore forced to produce high currents, a rapid voltage decline was observed, which corresponded to a rise in anodic potential, [54]. Local substrate consumption leading to a gradual decrease in biomass, and thus in voltage output, has also been reported for the case of organic-rich soils and graphite felt electrodes [55].
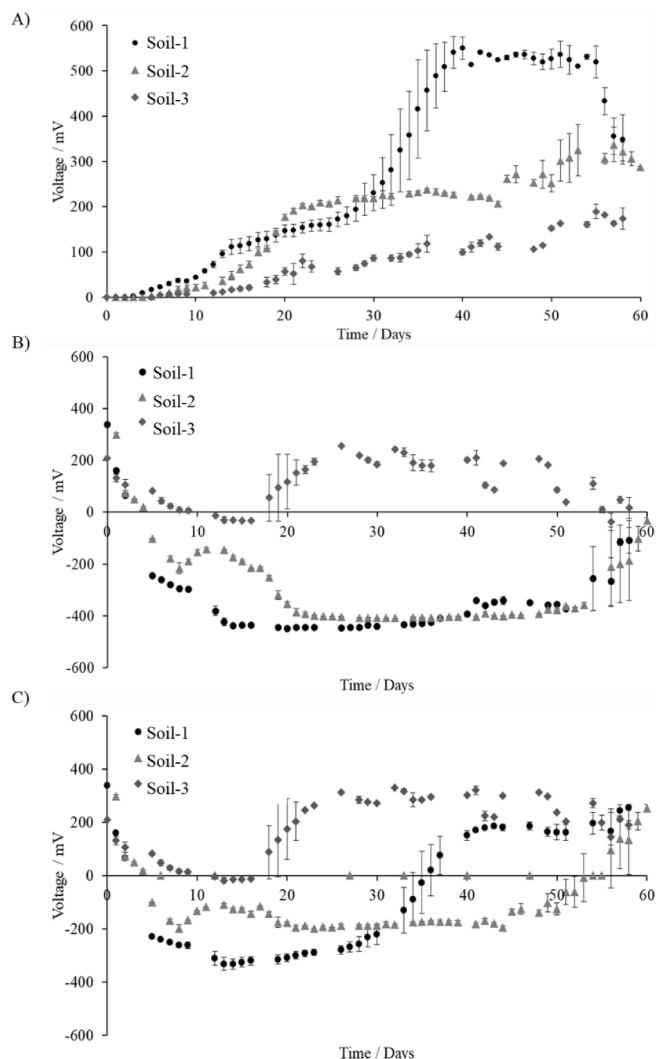

Fig. 4. Evolution of cell voltage and electrode potentials in SMFCs operated in three different quality soil. A) SMFC cell voltage; B) Anode potentials vs Ag/AgCl; C) Cathode potentials vs Ag/AgCl. Error bars refer to 3 replicates.

Influence of the soil quality

The electrochemical performance of SMFCs is clearly influenced by the physiochemical properties of the soil in which they are operated [56]. An in-depth investigation into the influence of soil type onto the enrichment process in SMFCs is, however, still missing. In this study, SMFCs were operated in three different soils, which mainly differ in their content of organic matter and permeability (see Table 1). Fig. 4A compares the enrichment curves of the SMFCs observed in the three soils over a 60-day period of operation.

As shown, in Soil-1, a steady voltage develops 4 and 10 days faster than in Soil-2 and Soil-3 respectively. This difference is associated to a faster drop in the anode potential in Soil-1 (Fig. 4B), which on day 10 reaches a value of −300 mV compared to −215 mV and 10 mV in Soil-2 and Soil-3 respectively. The most negative value of the anodic potential was −438 mV on day 15 in Soil-1, −392 mV on day 23 in Soil-2, and −33 mV on day 19 in Soil-3. Additionally, the negative anode potential was sustained the longest in Soil-1 (37 days), then in Soil-2 (30 days) and the shortest in Soil-3 (4 days).

This difference in the anode performance is aligned with the physiochemical differences of the three soil types tested. Soil-1 had the highest clay content (18 %), followed by Soil-2 (11 %) and Soil-3 (3 %). High clay content makes Soil-1 less permeable to oxygen, hence more

Table 2
Model parameters.

Symbol	Value	Unit	Ref.
$\mathscr{D}_S$	$1 \bullet 10^{-9}$	$m^2 s^{-1}$	[63]
$\mathscr{D}_{H^+}$	$9 \bullet 10^{-9}$	$m^2 s^{-1}$	[63]
$\mathscr{D}_{H^+}$	$5.3 \bullet 10^{-9}$	$m^2 s^{-1}$	[63]
$\mathscr{D}_{M_S}$	$3 \bullet 10^{-10}$	$m^2 s^{-1}$	[64]
$k_{1,An}$	$9.5 \bullet 10^{-7}$	$mol\,m^{-3}s^{-1}$	This work
$k_{2,An}$	$7.4 \bullet 10^{-4}$	$mol\,m^{-3}s^{-1}$	This work
$k_{1,Cat}$	$1 \bullet 10^{-6}$	$mol\,m^{-3}s^{-1}$	This work
$k_{2,Cat}$	4.25	$mol\,m^{-3}s^{-1}$	This work
$k_{d,An,Cat}$	1	d^{-1}	This work
K_{s,M_A}	34	$mol_C m^{-3}$	This work
K_{s,M_S}	2	$mol_C m^{-3}$	This work
$K_{s,S}$	60	$mol_C m^{-3}$	This work

anaerobic, which may be the reason for the faster drop in the anode potential and the sustained lower anode potential, and thus higher voltage generation, throughout the operation. Clay has been shown to be more promising than sand and silt for the operation of SMFCs, because of its membrane-like properties that restrict oxygen access to the anodic region while facilitating ion transfer [26,57].

As shown in Fig. 4C, in Soil-3 the cathode potential stabilised at + 312.5 mV, higher than that observed in Soil-1 (+186 mV) and Soil-2 (+140 mV), which was reached 14 and 31 days faster respectively. This evolving positive cathode potential in Soil-3 is, however, the consequence of a poorly performing anode, resulting in a poor electron transfer and accumulation at the cathode. Therefore, despite the highest cathodic potential, the SMFCs operated in Soil-3 generated the lowest maximum output voltage of 200 mV, compared to 550 mV in Soil-1, and 320 mV in Soil-3.

The difference in the organic content in the three types of soil is likely to be the main reason for the observed difference in the performance of the SMFCs. Organic matter content has a predominant influence on output voltage and power in microbial fuel cells [58]. On the other hand, the decrease in the voltage observed during Stage IV, may be attributed to substrate depletion nearby the anode [59], or in the bulk of

the soil [55,60]. Soil porosity, which influences the substrate mobility availability for the bio-electrochemical reactions, may dictate the relevance of either local or bulk substrate depletion at the anode. Soil-1 has an amount of organic matter respectively 2.6 and 5 times higher than Soil-2 and Soil-3. This suggests that the availability of fuel for the anodic biofilm is significantly higher in Soil-1, which is reflected by a more negative anode potential in this soil, sustained for a longer operating period. Additionally, the carbon to nitrogen ratio in soil can influence the metabolic activity of microbes [61] and it has demonstrated to affect the electrochemical performance of microbial fuel cells [62]. The C:N ratio in Soil-1 Soil-2 and Soil-3, derived from the total organic carbon and total nitrogen content (Table 1), is respectively 14:1, 13:1 and 10:1. Therefore, the higher C:N ratio in Soil-1 may have promoted a better anodic performance and greater voltage generation in Soil-1.

Computational model

The SMFCs were mathematically modelled to quantify the effect of different factors in soil that influence SMFC performance, and consequently derive guidelines on effective operating conditions and optimal electrode enrichment strategies.

A previously developed model [29] was adapted to interpret the experimental data, by introducing two processes at the cathode: a chemically catalysed ORR and a biologically catalysed ORR. Considering the complexity of soil matrices, a measurement of soil parameters during SMFC operation would require a great number of samples and/or online analyses to account for variations in time and space, which would ultimately be impractical with SMFC operations. We therefore based our model on a minimum number of experimental data, related to the most influential parameters, and derived the other data from the literature. The model was solved in three scenarios, corresponding to the three types of soil tested in the experiment, Soil-1, Soil-2 and Soil-3. The model parameters, summarised in Table 2, were derived from the experimental data (Fig. 5) and from the literature, as specified in Table 2.

The model parameters were determined from data of Soil-1; the trend with time of cell voltage was calculated with parameters from reference [22]. Kinetic constants were then adjusted to fit the experimental data. The same kinetic parameters were then used to model the
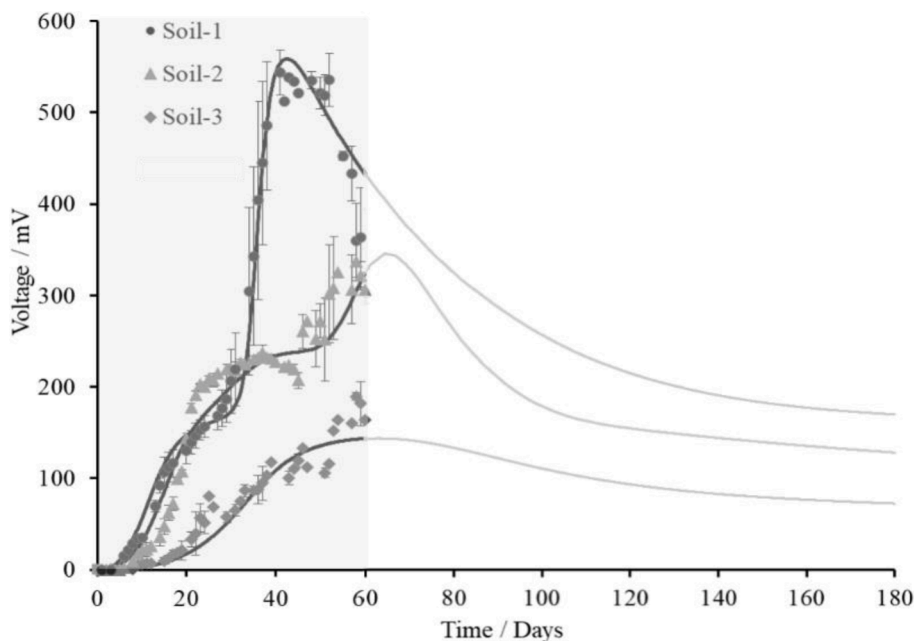

Fig. 5. Voltage evolution with time as predicted by the developed model up to 180 days of operation in the three different types of soil. Shaded area shows the model fit of the experimental data. Unshaded area shows the model prediction.
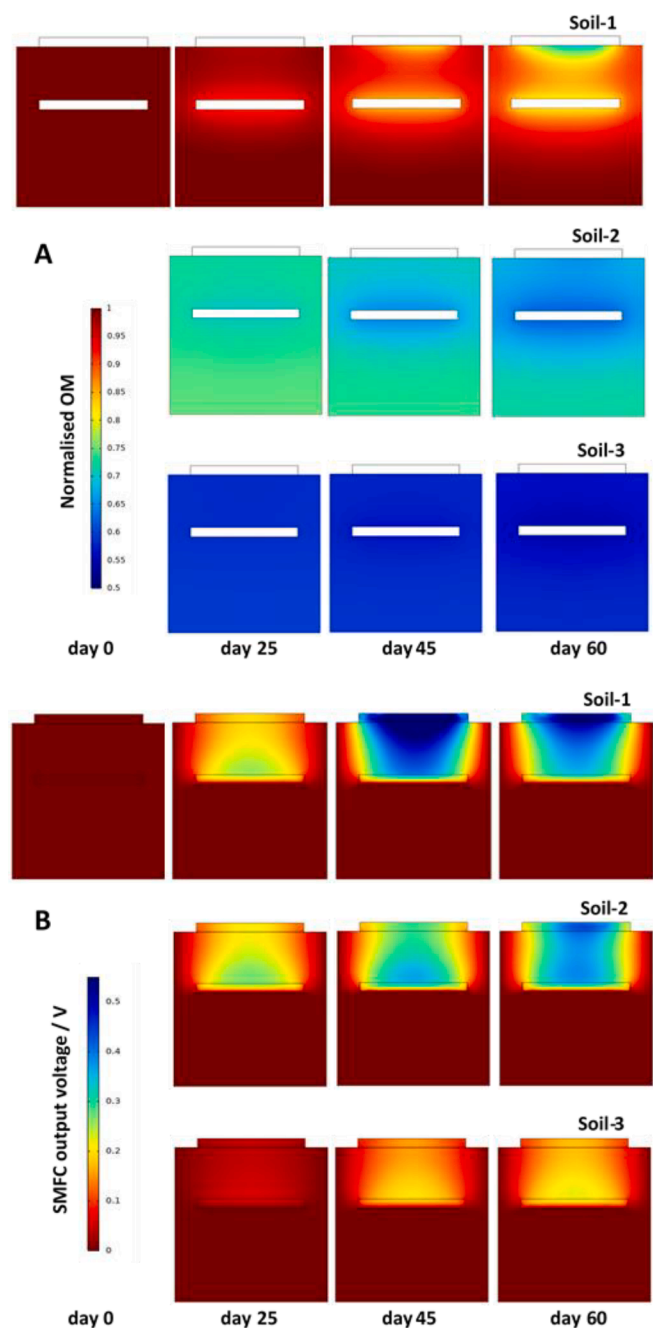
Fig. 6. Profiles of A) substrate (organic matter, OM) concentration, normalised with the initial values of each soil sample according to Table 1; and B) output voltage generated by the SMFCs operated in the three different types of soil, as predicted by the model, for times: 0 d, 25 d, 45 d, 60 d.

SMFCs in the other two types of soil, while the porosity and the organic content was changed to reflect the different properties in the three soil types tested. Values of porosity from the literature were used in the model, related to soils with the same content of sand, loam, clay, and organic matter of the samples used in the experiments: $\varepsilon = 0.3$ (Soil-1), and $\varepsilon = 0.6$ (Soil-2 and Soil-3) [65].

As shown in Fig. 5, the developed model can predict the experimental data obtained with the SMFCs operated in the three types of soil. The distribution of relative errors (as ratio RE between absolute error and experimental value) for Soil-1 shows that 87 % of each data prediction in the model has an RE lower than 10 %, while 78 % has an RE lower than 5 %. The corresponding values for the other soil types are: 83 % of prediction with RE < 10 % and 72 % with RE < 5 % (Soil-2); 78

% of prediction with RE < 10 % and 65 % with RE < 5 % (Soil-2).

Although the model underestimates the second value of plateau in the voltage, the difference between experimental and calculated data is within the experimental error for most data. In the case of the SMFCs operated in Soil-1, after a lag time of about 3 days, which depends on nucleation rate of the anodic biofilm (Equation (1)), the output voltage raises as current is generated through the mechanism described by Equation (2). After approximately 30 days of operation, the model predicts a second increase in the output voltage, corresponding this time to nucleation and growth of the cathodic biofilm, once again as described by Equation (1) and Equation (2) respectively; the potential then drops down after about 40 days. The model predicts a different trend of potential for the SMFC operated in Soil-2: the anodic biofilm nucleates and grows, leading to an increase in the SMFC output voltage, however the cathodic biofilm grows only after 50 days. When the SMFC is operated in Soil-3, a single increase in voltage is predicted.

The model can provide a quantitative interpretation of the effect that key soil properties, such as organic content and porosity, have on the electrochemical performance of the SMFCs. Fig. 6 shows the predicted space profiles of voltage and substrate concentration, normalised by the initial content of organic matter in the three soil types, under different operating times.

As shown, the model predicts clear differences among the three operating conditions. Soil-1 is characterised by high content of organics, and therefore by a great availability of substrate. This availability supports the bio-electrochemical reactions and allows the cell voltage to reach the value of about 150 V, corresponding to an anodic potential of −400 V, which favours the formation of the cathodic biofilm. On the other hand, Soil-1 has a low porosity, which influences the permeability of the soil, and therefore the ability of the substrate to diffuse towards the electrodes. The mobility of the substrate and ions is relatively low, and a local depletion of substrate is predicted near the electrodes under long operation times. As predicted by the Nernst-Monod mechanism, the substrate becomes limiting, and the growth rate of electroactive bacteria decreases, resulting in an overall decrease in biomass and, ultimately, in the output voltage.

Soil-2 has a lower content of organic matter with respect to Soil-1, but a higher porosity and therefore availability of organics. In this soil therefore, substrate consumption is initially balanced by the substrate diffusing from the bulk of the soil to the anode. Under longer operating times, the lower concentration of substrate in Soil-2, however, results in lower reaction rates, so that the growth of the cathodic biofilm is delayed to an operating time of over 50 days.

The availability of substrate is very high in Soil-3, since it is characterised by the largest porosity, however the content of soluble organics, and thus the reaction rates, is 5 times lower than the case of Soil-1. Consequently, the electricity generation is limited and so is the development of the cathodic biofilm.

The model also allows a prediction on performance according to the electrode distance in alignment with previous studies [66].

The formation of the cathodic biofilm depends on the cell potential, and then on the reaction rates. If the concentration of substrate available for the electricity generation is low, then the reaction rates, and the consequent raise of potential, are slow. Consequently, the formation of the cathodic biofilm could not start in Soil-3, or may require a much longer period to develop. These remarks are illustrated in Fig. 5, where the trends of voltage predicted by the model for up to 180 days are reported. Cathodic electrogenic activity is predicted for the SMFCs operated in Soil-1 and Soil-2, at long durations, whereas none is predicted for the case of Soil-3.

The model prediction of voltage decay over time raises concerns about the feasibility of SMFC technology in long-term implementations. The possibility of recovering the voltage was investigated for the SMFCs operated in Soil-1. In this case, the voltage decrease, occurring between day 52 and day 55, was accompanied by voltage fluctuations, which were caused by the anode. One hypothesis is that the high current
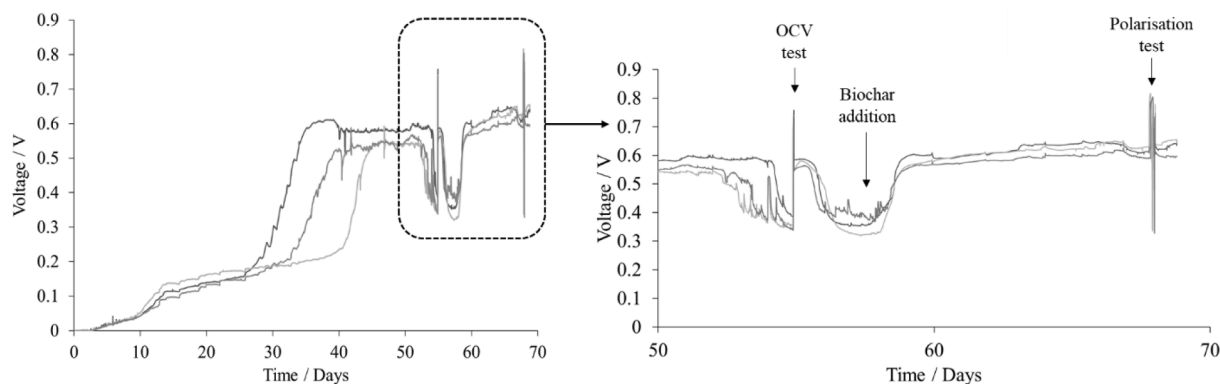
Fig. 7. Voltage recovery for the three SMFC replicates operated in Soil-1, with the addition of biochar. Data displayed shows a 1-minute sampling frequency of the fuel cell voltage.

generation exerted stress on the anodic biofilm, leading to performance disruption [67]. On day 55, the external load was disconnected and the SMFCs were left open circuit for 2 h, reaching an OCV of approximately 740 mV. After closing the circuit, the fuel cells generated an output potential of 550 mV, however, 12 h later the voltage dropped, and fluctuations in the anodic potential were observed (Fig. 7). To assess whether the voltage drop was related to substrate limitation, on day 57, 50 g of biochar was spread on top of the soil surface, as described in the methodology. One day later, a 200 mV rise in voltage was observed, and the SMFCs were able to sustain a steady voltage for another week, after which the study was stopped. This test confirms that the SMFC performance can be sustained provided that adequate organic matter is supplied. This can also be achieved by introducing plants in the soil, which deposit organics during photosynthesis [68].

Conclusions

SMFCs could play an important role in the space of renewable energy technologies if their performance can be controlled and engineered. In this regard, this study investigates the effect that physicochemical properties of the soil has on the performance of SMFCs, and accordingly presents operating conditions that ensure sustained energy generation. SMFCs operated in soil with greater clay content (less permeable to oxygen), developed a high voltage faster, due to a more rapid drop in the anodic potential. Additionally, for the first time, it has been shown that a well-functioning anode, with a negative potential of −450 mV, can boost the performance of the cathode (from −300 mV to + 180 mV), likely to be related to the growth of a catalytic biofilm onto the cathode surface, which leads to a substantial increase in the SMFC output voltage, under closed circuit conditions. Aside from soil porosity, the organic matter content is also critical. SMFC operated in soil with the highest organic matter content (50 %) significantly outperformed SMFCs in soils with 19 % and 10 % organic matter, generating 550 mV vs 320 mV and 200 mV, respectively. When local substrate depletion caused a drop in performance, the addition of biochar in soil was beneficial. The experimental data were used to develop a computational model that accurately predicts the SMFC performance according to soil conditions and becomes therefore a benchmark guide on how to effectively operate the technology and to guarantee optimal performance.

CRediT authorship contribution statement

Jakub Dziegielowski: Conceptualization, Data curation, Formal analysis, Investigation, Methodology, Validation, Visualization, Writing – original draft. **Michele Mascia:** Data curation, Formal analysis, Investigation, Methodology, Funding acquisition, Supervision, Project administration, Validation, Visualization, Writing – review & editing. **Benjamin Metcalfe:** Writing – review & editing. **Mirella Di Lorenzo:** Conceptualization, Funding acquisition, Supervision, Project administration, Validation, Visualization, Writing – review & editing.

Declaration of Competing Interest

The authors declare that they have no known competing financial interests or personal relationships that could have appeared to influence the work reported in this paper.

Data availability

Data will be made available on request.

References

[1] IEA. Global Energy Review 2022021.
[2] Alper K, Tekin K, Karagöz S, Ragauskas AJ. Sustainable energy and fuels from biomass: a review focusing on hydrothermal biomass processing. Sustainable. Energy Fuel 2020;4(9):4390–414.
[3] Gielen D, Boshell F, Saygin D, Bazilian MD, Wagner N, Gorini R. The role of renewable energy in the global energy transformation. Energ Strat Rev 2019;24: 38–50.
[4] Logan BE, editor. Microbial Fuel Cells. Hoboken, NJ, USA: John Wiley & Sons, Inc.; 2007.
[5] Santoro C, Arbizzani C, Erable B, Ieropoulos I. Microbial fuel cells: From fundamentals to applications. A review Journal of Power Sources 2017;356: 225–44.
[6] Wang H, Lu Lu, Mao D, Huang Z, Cui Y, Jin S, et al. Dominance of electroactive microbiomes in bioelectrochemical remediation of hydrocarbon-contaminated soils with different textures. Chemosphere 2019;235:776–84.
[7] Dziegielowski J, Bregu G, Hulse L, Di Lorenzo M, Cigolotti V. Assessing the effect of the electrode orientation on the performance of soil microbial fuel cells. E3S Web of Conferences 2022;334:08003.
[8] Michie I, Kim JR, Dinsdale RM, Guwy A, Premier GC. Factors affecting microbial fuel cell acclimation and operation in temperate climates. Water Sci Technol 2013; 11(67):2568–75.
[9] Molognoni D, Puig S, Balaguer MD, Liberale A, Capodaglio AG, Callegari A, et al. Reducing start-up time and minimizing energy losses of Microbial Fuel Cells using Maximum Power Point Tracking strategy. J Power Sources 2014;269:403–11.
[10] Gajda I, Greenman J, Ieropoulos I. Recent advancements in real-world microbial fuel cell applications. Curr Opin Electrochem 2018;11:78–83.
[11] Babauta J, Renslow R, Lewandowski Z, Beyenal H. Electrochemically active biofilms: facts and fiction. A review. Biofouling 2012;8(28):789–812.

[12] Aelterman P, Freguia S, Keller J, Verstraete W, Rabaey K. The anode potential regulates bacterial activity in microbial fuel cells. Applied Microbiological. Biotechnology 2008;3(78):409–18.

[13] Pasternak G, Greenman J, Ieropoulos I. Dynamic evolution of anodic biofilm when maturing under different external resistive loads in microbial fuel cells. Electrochemical perspective. J Power Sources 2018;400:392–401.

[14] Liu T, Yu Y, Li D, Song H, Yan X, Chen WN. The effect of external resistance on biofilm formation and internal resistance in Shewanella inoculated microbial fuel cells. RSC Adv 2016;6(24):20317–23.

[15] Zhang X, Li X, Zhao X, Li Y. Factors affecting the efficiency of a bioelectrochemical system: a review. Royal Society of Chemistry 2019;9(34):19748–61.

[16] Wang H, Luo H, Fallgren PH, Jin S, Ren ZJ. Bioelectrochemical system platform for sustainable environmental remediation and energy generation. Biotechnol Adv 2015;33(3–4):317–34.

[17] Li X, Wang X, Weng L, Zhou Q, Li Y. Microbial Fuel Cells for Organic-Contaminated Soil Remedial Applications: A Review. Energy Technology 2017;5(8):1156–64.

[19] Liang Y, Zhai H, Wang R, Guo Y, Ji M. Effects of water flow on performance of soil microbial fuel cells: Electricity generation, benzo[a]pyrene removal, microbial community and molecular ecological networks. Environ Res 2021;202:111658.

[20] Agriculture USDo. Natural Resources Conservation Service: Soil Texture Calculator. United States.

[21] Ministry of Agriculture FaFM. Agricultural Land Classification of England and Wales: Revised criteria for grading the quality of agricultural land (ALC011). England, UK1988.

[22] Dziegielowski J, Metcalfe B, Villegas-Guzman P, Martínez-Huitle CA, Gorayeb A, Wenk J, et al. Development of a functional stack of soil microbial fuel cells to power a water treatment reactor: From the lab to field trials in North East Brazil. Appl Energy 2020;278:115680.

[23] Monasterio Martinez S, Di Lorenzo M. Electricity generation from untreated fresh digestate with a cost-effective array of floating microbial fuel cells. Chem Eng Sci 2019;198:108–16.

[24] Backer R, Ghidotti M, Schwinghamer T, Saeed W, Grenier C, Dion-Laplante C, et al. Getting to the root of the matter: Water-soluble and volatile components in thermally-treated biosolids and biochar differentially regulate maize (Zea mays) seedling growth. PLoS One 2018;13(11):e0206924.

[25] A.G. Rombola, C. Torri, I. Vassura, E. Venturini, R. Reggiani, Fabbri D. Effect of biochar amendment on organic matter and dissolved organic matter composition of agricultural soils from a two-year field experiemnt. Science of The Total Environment. 2022;812:151422.

[26] Wetser K, Dieleman K, Buisman C, Strik D. Electricity from wetlands: Tubular plant microbial fuels with silicone gas-diffusion biocathodes. Appl Energy 2017;185: 642–9.

[27] Patwardhan SB, Pandit S, Kumar Gupta P, Kumar Jha N, Rawat J, Joshi HC, et al. Recent advances in the application of biochar in microbial electrochemical cells. Fuel 2022;311:122501.

[28] G. Papaharalabos, Stinchcombe A, Horsfield I, Melhuish C, Greenman J, Ieropoulos I. Autonomous Energy Harvesting and Prevention of Cell Reversal in MFC Stacks. Journal of The Electrochemical Society. 2017;164:3047-51.

[29] Casula E, Kim B, Chesson H, Lorenzo MD, Mascia M. Modelling the influence of soil properties on performance and bioremediation ability of a pile of soil microbial fue cells. Electrochim Acta 2021;368.

[30] Troyer ID, Merckx R, Amery F, Smolders E. Factors Controlling the Dissolved Organic Matter Concentration in Pore Waters of Agricultural Soils. Vadose Zone Journal. 2014;13(7).

[31] Casula E, Molognoni D, Borràs E, Mascia M. 3D modelling of bioelectrochemical systems with brush anodes under fed-batch and flow conditions. J Power Sources 2021;487:229432.

[32] Marcus AK, Torres CI, Rittmann BE. Conduction-based modeling of the biofilm anode of a microbial fuel cell. Biotechnol Bioeng 2007;98(6):1171–82.

[33] Zeng Y, Choo YF, Kim BH, Wu P. Modelling and simulation of two-chamber microbial fuel cell. J Power Sources 2010;195(1):79–89.

[34] Mateo S, Mascia M, Fernandez-Morales FJ, Rodrigo MA, Lorenzo MD. Assessing the impact of design factors on the performance of two miniature microbial fuel cells. Electrochim Acta 2019;297:297–306.

[35] Seager RJ, Acevedo AJ, Spill F, Zaman MH. Solid dissolution in a fluid solvent is characterized by the interplay of surface area-dependent diffusion and physical fragmentation. Sci Rep 2018;8(7711).

[36] Picioreanu C, Head IM, Katuri KP, van Loosdrecht MC, Scott K. A computational model for biofilm-based microbial fuel cells. Water Res 2007;41(13):2921–40.

[37] Hashemi F, Rowshanzamir S, Rezakazemi M. CFD simulation of PEM fuel cell performance: Effect of straight and serpentine flow fields. Math Comput Model 2012;55(3):1540–57.

[38] Zhang Z, Furman A. Soil redox dynamics under hydrologic regimes- A review. Sci Total Environ 2021:763.

[39] A. Mahadevan, D.A. Gunawardena, Fernando S. Technology and Application of Microbial Fuel Cells. Wang C-T, editor2014.

[40] S. Li, Y.E. Song, J. Baek, H.S. Im, M. Sakuntala, M. Kim, et al. Bioelectrosynthetic Conversion of CO2 Using Different Redox Mediators: Electron and Carbon Balances in Bioelectrochemical Systems. Energies. 2020;13.

[41] Lee HS, Torres CI, Rittmann BE. Effects of Substrate Diffusion and Anode Potential on Kinetic Parameters for Anode-Respiring Bacteria. Environ Sci Tech 2009;43: 7571–7.

[42] Rismani-Yazdi H, Carver SM, Christy AD, Tuovinen OH. Cathodic limitations in microbial fuel cells: An overview. J Power Sources 2008;180(2):683–94.

[43] Garcia-Alcalde L, Gonzales Z, Barreda D, Rocha VG, Blanco C, Santamaria R. Unraveling the relevance of carbon felts surface modification during electrophoretic deposition of nanocarbons on their performance as electrodes for the VO2+ and VO2+ redox couple. Appl Surf Sci 2021:569.

[44] Dziegielowski J, Poyiatzi N, Lorenzo MD. Design Optimization of Soil Microbial Fuel Cells for Energy Harvesting in Remote Areas. Italy: European Fuel Cell Technology; Naples; 2019.

[45] Cheng Y, Chen H, Basurto LAS, Protasenko VV, Bharadwaj S, Islam M, et al. Inactivation of Listeria and E. coli by Deep-UV LED: effect of substrate conditions on inactivation kinetics. Sci Rep 2020;10(3411).

[46] Monasterio S, Lorenzo MD. Electricity generation from untreated fresh digestate with a cost-effective array of floating microbial fuel cells. Chem Eng Sci 2019;198: 108–16.

[47] He Z, Angenent LT. Application of Bacterial Biocathodes in Microbial Fuel Cells. Electroanalysis 2006;18:2009–15.

[48] Milner EM, Popescu D, Curtis T, Head IM, Scott K, Yu EH. Microbial fuel cells with highly active aerobic biocathodes. J Power Sources 2016;324:8–16.

[49] Electrochemical Investigation of Aerobic Biocathodes at Different Poised Potentials: Evidence for Mediated Extracellular Electron Transfer. Chemical Engineering Transactions; 2014. p. 41.

[50] Campo AGd, Canizares P, Lobato JL, Rodrigo M, Fernandez-Morales FJ. Effects of External Resistance on Microbial Fuel Cell's Performance. In: Springer, editor. Environment, Energy and Climate Change II2014.

[51] Margaria V, Tommasi T, Pentassuglia S, Agostino V, Sacco A, Armato C, et al. Effects of pH variations on anodic marine consortia in a dual chamber microbial fuel cell. Int J Hydrogen Energy 2017;42:1820–9.

[52] Yuan Y, Zhao B, Zhou S, Zhong S, Zhuang L. Electrocatalytic activity of anodic biofilm responses to pH changes in microbial fuel cells. Biosource Technology 2011;102:6887–91.

[53] Fischer F, Sugnaux M, Savy C, Hugenin G. Microbial fuel cell stack power to lithium battery stack: Pilot concept for scale up. Appl Energy 2018;230:1633–44.

[54] Dziegielowski J, Metcalfe B, Lorenzo MD. Towards effective energy harvesting from stacks of soil microbial fuel cells. J Power Sources 2021:515.

[55] Yu B, Feng L, He Y, Yang L, Xun Y. Effects of anode materials on the performance and anode microbial community of soil microbial fuel cell. J Hazard Mater 2021; 401(5).

[56] Huan D, Yi-Cheng W, Z-Fan, H. Zong-Chuan, C. Zheng, X. Hui-Juan,, et al. Factors Affecting the Performance of Single-Chamber Soil Microbial Fuel Cell for Power Generation. Pedosphere 2014;24(3):330–8.

[57] E. Fosso-Kankeu, S. Marx, F. Waanders, Jacobs V. Impact of soil type on electricity generation from a Microbial Fuel Cell. 7th International Conference on Latest Trends In Engineering & Technology; Pretoria (South Africa)2015.

[58] Y. Jiang, W.H. Zhong, C. Han, Deng H. Characterization of Electricity Generated by Soil Microbial Fuel Cells and the Isolation of Soil Source Exoelectrogenic Bacteria. Front Microbiol. 2016;7.

[59] Huang D, Zhou S, Chen Q, Zhao B, Yuan Y, Zhuang L. Enhanced anaerobic degradation of organic pollutants in a soil microbial fuel cell. Chem Eng J 2011; 172(2–3):647–53.

[60] Xu X, Zhao Q, Wu M, Ding J, Zhang W. Biodegradation of organic matter and anodic microbial communities analysis in sediment microbial fuel cells with/ without Fe(III) oxide addition. Bioresour Technol 2017;225:402–8.

[61] Khanal SK, Nindgia TGT. Nitayavardhana S. Biogas From Wastes: Processes and Applications. Sustainable Resource Recovery and Zero Waste Approaches; 2019. p. 165–74.

[62] Khudzari J, Tartakovsky B, Vijaya Raghavan GS. Effect of C/N ratio and salinity on power generation in compost microbial fuel cells. Waste Manag 2016;48:135–42.

[63] Korth B, Rosa LFM, Harnisch F, Picioreanu C. A framework for modeling electroactive microbial biofilms performing direct electron transfer. Bioelectrochemistry 2015;106:194–206.

[64] Kim Y-C. Diffusivity of bacteria. Korean J Chem Eng 1996;13(3):282–7.

[65] Martinez-Fernandez J, Gonzalez-Zamora A, Almendra-Martin L. Soil moisture memory and soil properties: An analysis with the stored precipitation fraction. J Hydrol 2021:593.

[66] Zhang X, Li X, Zhao X, Chen X, Zhou B, Weng L, et al. Bioelectric field accelerates the conversion of carbon and nitrogen in soil bioelectrochemical systems. J Hazard Mater 2020;388(121790).

[67] An J, Sim J, Lee H. Control of voltage reversal in serially stacked microbial fuel cells through manipulating current: Significance of critical current density. J Power Sources 2015;283:19–23.

[68] Nitisoravut R, Regmi R. Plant microbial fuel cells: A promising biosystems engineering. Renew Sustain Energy Rev 2017;76:81–9.

Further reading

[18] Abbas SZ, Rafatullah M. Recent advances in soil microbial fuel cells for soil contaminants remediation. Chemosphere 2021;272:129691.